APPLIED PHYSICS LETTERS **86**, 183501 (2005)

Generation of high-confinement step-like optical waveguides in $LiNbO_3$ by swift heavy ion-beam irradiation

J. Olivares[a)]
Instituto de Optica "Daza de Valdés," CSIC, C/Serrano 121, 28006-Madrid, Spain

G. García, A. García-Navarro, and F. Agulló-López[b)]
Centro de Microanálisis de Materiales (CMAM), Universidad Autonoma de Madrid, Cantoblanco 28049-Madrid, Spain

O. Caballero and A. García-Cabañes
Departamento de Física de Materiales, Universidad Autonoma de Madrid, Cantoblanco 28049-Madrid, Spain

(Received 27 January 2005; accepted 4 April 2005; published online 26 April 2005)

We demonstrate a swift ion-beam irradiation procedure based on electronic (not nuclear) excitation to generate a large index jump step-like optical waveguide ($\Delta n_0 \approx 0.2$, $\Delta n_e \approx 0.1$) in $LiNbO_3$. The method uses medium-mass ions with a kinetic energy high enough to assure that their electronic stopping power $S_e(z)$ reaches a maximum value close to the amorphous (latent) track threshold inside the crystal. Fluorine ions of 20 and 22 MeV and fluences in the range $(1-30)\times 10^{14}$ are used for this work. A buried amorphous layer having a low refractive index (2.10 at a wavelength of 633 nm) is then generated at a controlled depth in $LiNbO_3$, whose thickness is also tuned by irradiation fluence. The layer left at the surface remains crystalline and constitutes the core of the optical waveguide which, moreover, is several microns far from the end of the ion range. The waveguides show, after annealing at 300 °C, low propagation losses ($\approx$1 dB/cm) and a high second-harmonic generation coefficient (50%–80% of that for bulk unirradiated $LiNbO_3$, depending on the fluence). The formation and structure of the amorphous layer has been monitored by additional Rutherford backscattering/channeling experiments. © *2005 American Institute of Physics*. [DOI: 10.1063/1.1922082]

Ion implantation of light ions (H and He) has been extensively investigated[1] as an alternative to classical methods, impurity diffusion and ion exchange, to fabricate optical waveguides in dielectric and electro-optic materials, such as $LiNbO_3$. It has the advantage of being a flexible universal method. However, the obtained refractive index profiles that are based on nuclear collision damage are smooth and typically require very high irradiation fluences ($10^{16}-10^{17}$ cm^{-2}). Recently, the use of heavier ions and higher energies to obtain waveguides is starting to be explored. Silicon,[2] nickel[3] at 3 MeV, and oxygen,[4] fluorine,[5] and nitrogen[5] irradiations at around 5 MeV have already been investigated. The fluences needed to achieve waveguiding are markedly reduced down to around 10^{14} cm^{-2}. However, the refractive index changes are neither large nor sharp, and their origin is not well understood. Although the nuclear collision damage still seems to be responsible for a significant part of the refractive index modification in the low-energy range, it has been pointed out that electronic excitation could also be used to generate structural changes (and/or damage) and modify the refractive indices.[4–6] Particularly, oxygen and fluorine ions of 5 MeV generate a heavily damaged layer at the surface after some critical fluence of $(2-6)\times 10^{14}$ cm^{-2}. Moreover, using silicon ions of 5 and 8 MeV, it has been recently found that such a surface layer is optically isotropic and presents a low refractive index (i.e., amorphous-like), and that its thickness increases with fluence.[6] The physical basis recalled to explain the process is as follows: lattice amorphization is induced[7,8] along the trajectories of bombarding ions whenever the electronic stopping power S_e is above a certain threshold $S_{e,\mathrm{th}}$. The so-called latent tracks have a diameter of around a few nanometers. When the irradiation fluence assures full overlapping of the individual tracks, a homogeneous amorphous layer is generated.

In this letter, we propose and implement a method, based on the electronic excitation mechanism just described, to fabricate an optical waveguide by means of choosing the experimental irradiation conditions (type of ion, high enough energy) so that the maximum electronic stopping power (above or close to the threshold for electronic-induced amorphization) lies inside the crystal and not at the surface. An optically isotropic low-refractive-index (amorphous-like) region is then generated inside the crystal, whereas the material remains crystalline near the surface. The high-index crystalline layer at the surface constitutes the core of an optical waveguide. Conceptually the procedure relies on the same optical barrier scheme successfully applied with light-ion implantation, but using the more effective (as it has turned out to be) electronic excitation. Moreover, the waveguide is several microns far from the end of range, thus keeping the impurity level at a minimum. The method has been specifically applied to $LiNbO_3$, which is a reference material[9] for electro-optic and nonlinear optical (NLO) applications.

X- and *Z*-cut nominally pure (integrated optical grade) $LiNbO_3$ plates purchased from Photox Optical Systems, UK,

[a)]Electronic mail: j.olivares@io.cfmac.csic.es
[b)]Also at: Departamento de Física de Materiales, Universidad Autonoma de Madrid, Cantoblanco 28049-Madrid, Spain

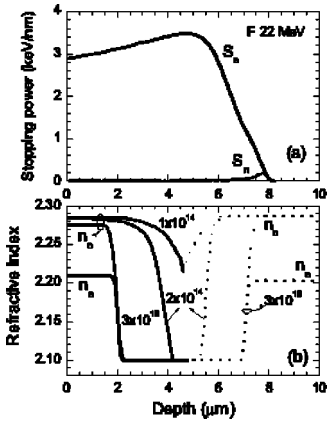

FIG. 1. (a) Electronic (S_e) and nuclear (S_n) stopping power of 22-MeV fluorine ions in $LiNbO_3$ calculated with SRIM 2003. (b) Ordinary (n_o) and extraordinary (n_e) refractive index profiles obtained from the dark-mode data (solid lines) for some representative fluences. The estimated refractive index profile (using the low-index optical resonances and RBS/channeling data) corresponding to the back amorphous-crystalline boundary is also shown with dashed lines.

were irradiated with F^{+4} ions at 20 and 22 MeV in the 5 MV tandetron accelerator recently installed at the CMAM in the University Autónoma de Madrid.[10] The samples were tilted 8° relative to normal incidence to avoid channeling and the beam current density was kept below 200 nA/cm^2 to minimize charging and heating. In order to characterize the structural changes induced in the irradiated samples Rutherford backscattering (RBS)/channeling experiments were performed along the *c*-axis channel using H ions at 3 MeV. The waveguide modes have been characterized by the prism-coupling dark *m*-lines technique using a 5 mW He–Ne laser ($\lambda = 632.8$ nm). Propagation losses were determined by measuring the scattered laser light along the beam trajectory in the waveguide with a CCD camera. The second-harmonic (SH) response was evaluated by using the method described in Ref. 11 and applied to proton-exchange waveguides. As a fundamental beam the 532 nm output (ns pulses) of a frequency-doubled Nd:YAG laser was focused on the irradiated surface of the plate to an intensity of 10^{12} W m^{-2} to generate a SH beam at 266 nm. The light polarization is chosen to probe the d_{33} coefficient.

In this work, the selected energy of the ion irradiation is substantially higher than those previously used in implantation experiments both to assure the dominant effect of electronic excitation in waveguide formation and to have the maximum of the electronic stopping buried a few microns inside the crystal. In fact, the physical situation achieved during irradiation is illustrated in Fig. 1(a) showing the results of SRIM 2003 calculations for the nuclear (S_n) and electronic (S_e) stopping powers for 22-MeV fluorine ions. The maximum of the $S_e(z)$ curve is inside the crystal at a depth of about 4.5 μm, well separated from the peak value of the nuclear stopping power S_n at the end of the ion range ($z \approx 8$ μm). The generated waveguides show several sharp dark modes for both ordinary and extraordinary polarizations for fluences above a threshold value of 1×10^{14} cm^{-2}. The measured values of the effective refractive index squared (N_m^2) are shown in Fig. 2 as a function of m^2, *m* being the mode order, for the various obtained modes. The obtained refractive index profile for some representative fluences are illustrated in Fig. 1(b). The data corresponding to the threshold fluence (1×10^{14} cm^{-2}) indicate a maximum waveguide thickness (i.e., maximum damage depth) at around 4.5 μm, in very good agreement with the maximum of $S_e(z)$, clearly supporting the hypothesis of electronic induced amorphization. For fluences above 2×10^{14} cm^{-2} the measured N_m^2 approximately follow a $N_m^2 \propto m^2$ dependence, as it is shown in Fig. 2, indicating that an approximate step-like index profile has been generated at the surface. The upper values of the step profiles are consistent with those for the bulk crystal (Table I). The bottom level of the refractive index step is obtained from the abrupt change in slope of the $N_m^2 \propto m^2$ plot. It is approximately the same for the two polarizations and coincides with the refractive index of amorphous $LiNbO_3$ (Refs. 6 and 12) ($n_a = 2.10$). The thickness of the waveguiding layer determined from the optical measurements is a function of the irradiation fluence ϕ, as it is clearly seen in Fig. 2 and given in Table I. It reveals that the position of the (front) boundary separating the crystalline and amorphous layers moves towards the input surface of the sample on increasing fluence. On the other hand, for $N_m < n_a$ some resonances are also measured which are caused by the refractive index jump at the back amorphous-crystalline boundary as indicated by the much smaller slope in Fig. 2. RBS/channeling data shown below also indicate that the back boundary moves towards the end of ion range. Given the relevance for the waveguide performance (i.e., high mode confinement allowing the production of nonleaky narrow monomode waveguides) this estimated part of the refractive index profile has also been plotted in Fig. 1(b) with dashed lines (the expected refractive index change in the nuclear stopping layer, not relevant for this work, is neglected). This boundary motion effect has been recently observed and attributed to a reduction in the amorphization threshold with fluence.[6] Note that optical barriers as wide as 4–5 μm are obtained for fluences of $\sim 1 \times 10^{15}$ cm^{-2}.

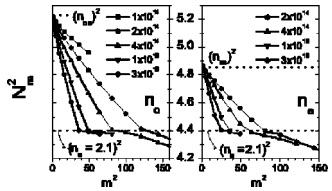

FIG. 2. Effective refractive index squared (N_m^2) of the measured modes and resonances as a function of the mode number squared (m^2) for ordinary (left) and extraordinary (right) polarization, for the fluences indicated in the figure. The squared refractive indices for the bulk $LiNbO_3$ and for amorphous layer are also indicated with dashed lines.

TABLE I. Data for the *Z*-cut samples irradiated with 22-MeV F ions. h_{opt} and h_{RBS} are, respectively, the waveguide thickness obtained from the dark-mode optical measurements and from the RBS/channeling measurements. $n_{e,s}$ and $n_{o,s}$ refer to the surface refractive index for extraordinary and ordinary polarization, respectively. $\chi_{33}^{(2)}$(norm) stands for the second-order susceptibility measured relative to a virgin substrate.

Fluence (at/cm^{-2})	h_{opt} (μm)	h_{RBS} (μm)	$n_{e,s}$	$n_{o,s}$	$\chi_{33}^{(2)}$(norm)
1×10^{14}	4.5	3.7	⋯	2.286	0.8
2×10^{14}	3.6	2.7	2.207	2.284	0.7
4×10^{14}	3.0	2.3	2.208	2.281	0.6
1×10^{15}	2.3	1.8	2.210	2.278	0.6
3×10^{15}	2.0	1.6	2.211	2.278	0.5

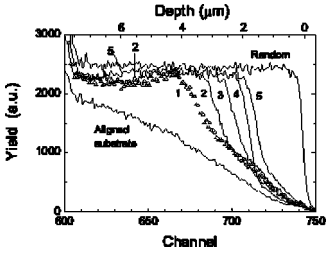

FIG. 3. RBS/channeling spectra measured, with 3-MeV H along the *c* axis, in *Z*-cut samples irradiated with 22-MeV F ions at the fluences of (1) 1×10^{14} (triangles symbols), (2) 2×10^{14}, (3) 4×10^{14}, (4) 1×10^{15}, and (5) 3×10^{15}. For the purposes of clarity, only the spectra corresponding to curves (2) and (5) are plotted for channels below 700. The depth scale shown has been calculated using the density of the virgin $LiNbO_3$; it understimates the width of the buried amorphous layer since it is expected to have a lower density.

Figure 3 shows the RBS/channeling data taken by using 3-MeV H as probing ions on the irradiated *z*-cut samples. One sees that at fluences above 10^{14} cm^{-2} a buried region with random-like yield is observed. The thickness of the waveguide layer decreases as the buried damaged layer grows with fluence. Values are listed in Table I together with the optical data. The front crystalline-amorphous boundary is quite sharp in agreement with the optical (dark-mode data). On the other hand, the high-index surface layer shows relatively clean channeled spectra suggesting a good crystallinity and thus good optical properties.

Experimental data after implantation show high light propagation losses associated to color centers introduced during the irradiation. However, annealing treatments above 200 °C markedly improve the propagation, improving at the same time the sharpness of the refractive index step. It is noticeable that after 1 h annealing at 300 °C, the low refractive index of the amorphous layer remains unchanged. Figure 4 shows the losses measurement obtained for extraordinary-index propagation in an *X*-cut sample irradiated with 20 -MeV F ions at the intermediate fluence of 4×10^{14} cm^{-2} and annealed 1 h at 300 °C in air. The quantitative analysis of the scattered light shows losses around 1 dB/cm, which appears competitive with values reported for waveguides prepared by other implantation techniques.[2–5] In order to assess the potential of the generated waveguide for NLO devices the second-harmonic generation (SHG) response of the layer has been measured for several fluences. By comparing to a reference $LiNbO_3$ substrate, the SHG susceptibility of the waveguides at the crystal surface amounts to ≈80% of the bulk value of unirradiated $LiNbO_3$ for low fluences. For higher fluences a monotonic decrease is found as given in Table I. On the other hand, no substantial improvement is obtained after annealing at 300 °C. The decrease in SHG yield may be related to small structural disorder and to domain depolarization caused by the irradiation as previously reported for He^+ implantation in both $LiNbO_3$ (Ref. 13) and $KNbO_3$.[14] Further work on irradiation conditions, annealing, and domain poling is needed.

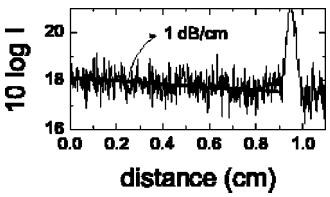

FIG. 4. Loss measurement derived from the scattered light from the fundamental extraordinary mode of a waveguide produced by irradiating an *X*-cut sample with 20-MeV F ions at a fluence of 4×10^{14} cm^{-2} and annealed in air 1 h at 300 °C. The strong peak is due to a scratch on the surface.

In summary, a sharp step-like optical waveguide has been generated at the surface by irradiating $LiNbO_3$ substrates with a 20–22 MeV F beam at fluences in the range 2×10^{14}–3×10^{15} cm^{-2}. At this energy, the electronic stopping power reaches a maximum beneath the surface, with a value close to the threshold for amorphization. A several-micron-wide isotropic ("amorphous") low-index layer ($n=2.10$ at $\lambda=633$ nm) is then created by the swift heavy ion-beam irradiation. The crystalline surface layer constitutes the waveguide core and approximately maintains the refractive index values of the bulk crystal. Therefore, large refractive index jumps of $\Delta n_o \approx 0.2$ and $\Delta n_e \approx 0.1$ are created, allowing for the propagation of highly confined modes. The high optical confinement, reasonable low waveguide losses (~1 dB/cm) and significant second-harmonic efficiency (about 50%–80% of that for unirradiated $LiNbO_3$) show a promising performance for optoelectronic applications. Furthermore, the method is expected to apply to other relevant crystalline materials.

We acknowledge the funding of the project MAT2002–03220 (MEC). A. García-Navarro acknowledges the financial support of the MEC through a FPU Fellowship and of the Madrid City Hall-Residencia de Estudiantes.

[1] P. D. Townsend, P. J. Chandler, and L. Zhang, *Optical Effects of Ion Implantation* (Cambridge University Press, Cambridge, 1994).
[2] H. Lu, F. Lu, F. Chen, B.-R. Shi, K.-M. Wang, and D.-Y. Shen, J. Appl. Phys. **89**, 5224 (2001).
[3] F. Lu, T. Zhang, X. Wang, S. Li, K. Wang, D. Shen, and H. Ma, J. Appl. Phys. **96**, 3463 (2004).
[4] G. G. Bentini, M. Bianconi, M. Chiarini, L. Correia, G. Sada, P. Mazzoldi, N. Argiolas, M. Basan, and R. Guzzi, J. Appl. Phys. **92**, 6477 (2002).
[5] G. G. Bentini, M. Bianconi, L. Correra, M. Chiarini, P. Mazzoldi, G. Sada, N. Argiolas, M. Bazzan, and R. Guzzi, J. Appl. Phys. **96**, 242 (2004).
[6] J. Olivares, G. García, F. Agulló-López, F. Agulló-Rueda, A. Kling, and J. C. Soares, Appl. Phys. A: Mater. Sci. Process. (in press).
[7] M. Toulemonde, S. Bouffard, and F. Studer, Nucl. Instrum. Methods Phys. Res. B **91**, 108 (1994).
[8] B. Canut and S. M. Ramos, Radiat. Eff. Defects Solids **145**, 1 (1998).
[9] *Properties of Lithium Niobate*, edited by K. K. Wong, EMIS Datareview Series (INSPEC, Exeter, 2002).
[10] D. J. W. Mous, A. Gottdang, R. G. Haitsma, G. García López, A. Climent-Font, F. Agulló-López, and D. O. Boerma, Proceedings CAARI 2002.
[11] J. Rams and J. M. Cabrera, J. Mod. Opt. **47**, 1659 (2000).
[12] G. L. Destefanis, G. P. Gailliard, E. L. Ligeon, S. Valette, B. W. Farmery, P. D. Townsend, and A. Perez, J. Appl. Phys. **50**, 7898 (1980).
[13] J. Rams, J. Olivares, P. J. Chandler, and P. D. Townsend, J. Appl. Phys. **84**, 5180 (1998).
[14] D. Fluck, T. Pliska, M. Küpfer, and P. Günter, Appl. Phys. Lett. **67**, 748 (1995).